Toxicology in Vitro 23 (2009) 1326–1332

Contents lists available at ScienceDirect

Toxicology in Vitro

journal homepage: www.elsevier.com/locate/toxinvit

Oxidative stress of silica nanoparticles in human bronchial epithelial cell, Beas-2B

Hyun-Jeong Eom, Jinhee Choi *

Faculty of Environmental Engineering, College of Urban Science, University of Seoul, 90 Jeonnong-dong, Dongdaemun-gu, Seoul 130-743, Korea

ARTICLE INFO

Article history:
Received 20 August 2008
Accepted 7 July 2009
Available online 12 July 2009

Keywords:
Silica nanoparticles
Oxidative stress
HO-1
Nrf-2
ERK

ABSTRACT

In this study, the potentially harmful effect of the exposure to fumed and porous silicon dioxide (silica) nanoparticles was investigated using human bronchial epithelial cell, Beas-2B, with a focus on the involvement of oxidative stress as the toxic mechanism. Silica nanoparticles-induced oxidative stress was assessed by examining the formation of reactive oxygen species (ROS) and induction of antioxidant enzymes, such as superoxide dismutase (SOD) and heme oxygenase-1 (HO-1). Subsequently, to understand the mechanism of nanoparticles-induced oxidative stress, the involvement of oxidative stress-responding transcription factors, such as, nuclear factor-kappaB (NF-κB) and nuclear factor-E2-related factor-2 (Nrf-2), as well as the mitogen-activated protein (MAP) kinase signal transduction pathway were investigated. From the overall results, silica nanoparticles exerted toxicity via oxidative stress, which lead to the induction of HO-1 via the Nrf-2–ERK MAP kinase signaling pathway; cells exposed to porous silica nanoparticles showed a more sensitive response than those exposed to fumed silica. Nevertheless, the parameters tested were rather limited in terms of gaining a full understanding of the oxidative stress and cellular response due to exposure to silica nanoparticles. Further studies on the mechanism by which silica nanoparticles induce the Nrf-2–ERK MAP kinase pathway, to more clearly elucidate the silica-induced oxidative stress, as well as on the relationship between the physico-chemical properties of nanoparticles and their cytotoxicity are warranted to gain an understanding of the phenomenon of different sensitivities between porous and fumed silica.

1. Introduction

Nanoparticle toxicity studies are among the fastest growing area of environmental toxicology research due to the fast applications of nanotechnology to a wide variety of fields (Nohynek et al., 2007; Rogueda and Traini, 2007; Warheit et al., 2007). Investigations into the potential health and environmental risks related to the widespread production and use of nanomaterials created by these technologies are increasing in terms of their toxic mechanism (Hoet et al., 2004; Oberdörster et al., 2005; Nel et al., 2006; Handy et al., 2008). Of the various manufactured nanomaterials, silicon dioxide (silica) has the potential for widespread applications. As a non-metal oxide, silica nanoparticles have found extensive applications in chemical mechanical polishing and as additives to drugs, cosmetics, printer toners, varnishes and food stuffs (Lu et al., 2007; Zhao et al., 2007). The use of silica nanoparticles has recently been extended to biomedical and biotechnological fields, such as biosensors for the simultaneous assay of glucose, lactate, L-glutamate and hypoxanthine in rat striatum (Zhang et al., 2004), biomarkers for leukemia cell identification using optical microscopy imaging (Santra et al., 2001), cancer therapy (Hirsch et al., 2003), DNA delivery (Bharali et al., 2005; Gemeinhart et al., 2005), drug delivery (Venkatesan et al., 2005) and enzyme immobilization (Qhobosheane et al., 2001).

Considering their wide range of applications, the impact of silica nanomaterials on human health and the environment is of great interest. In this study, the potential harmful effect of exposure to silica nanoparticles was investigated by conducting an *in vitro* toxicity assay focusing on the involvement of oxidative stress as the toxic mechanism. Although little is known about nanoparticle toxicity, oxidative stress has often been reported as a nanoparticle-induced toxicity. Oxidative stress, which elicits a wide variety of cellular events, such as apoptosis, cell cycle arrest and the induction of antioxidant enzymes, is thought to be involved in nanoparticle toxicity. Numerous previous studies on nanoparticle toxicity, with various cell types and nanoparticle types, reported that oxidative stress is one of the most important toxicity mechanisms related to nanoparticles exposure (Shvedova et al., 2003; Green and Howman, 2005; Lin et al., 2006; Monteiller et al., 2007). Indeed, previous studies have reported oxidative stress as the toxic mechanism of silica nanoparticles (Kaewamatawong et al., 2006; Lin et al., 2006).

In this study, to understand the potential harmful effect of nanoparticles on human health, the oxidative stress-related toxicity was investigated by exposure to silica nanoparticles. Human bronchial epithelial cells, Beas-2B, were selected because pulmonary exposure

* Corresponding author. Tel.: +82 2 2210 5622; fax: +82 2 2244 2245.
E-mail address: jinhchoi@uos.ac.kr (J. Choi).

0887-2333/$ - see front matter © 2009 Elsevier Ltd. All rights reserved.
doi:10.1016/j.tiv.2009.07.010

is an important pathway for exposure to silica nanoparticles. Oxidative stress was assessed by examining the formation of reactive oxygen species (ROS) and the induction of antioxidant enzyme, such as superoxide dismutase (SOD) and heme oxygenase-1 (HO-1). Subsequently, to understand the mechanism of nanoparticles-induced oxidative stress, the involvement of oxidative stress-responding transcription factors, and the signal transduction pathway in the toxicity of silica nanoparticles was also investigated.

Redox-sensitive transcription factors, such as nuclear factor-kappaB (NF-κB) and nuclear factor-E2-related factor-2 (Nrf-2), were investigated as target transcription factors of silica nanoparticles toxicities. NF-κB has been identified as a transcription factor regulated by the intracellular redox status, which is activated by oxidative stress and induces the expression of a variety of proteins that function in the immunological and cellular detoxifying defense systems (Janssen et al., 1995; Pinkus et al., 1996; Sen and Packer, 1996). Many studies have reported that the transcription factor Nrf-2 plays an essential role in the antioxidant response element (ARE)-mediated expression of antioxidant enzymes and other stress-inducible genes in response to oxidative stress (Itoh et al., 1997; Chan and Kan, 1999; Hayes et al., 2000; Chan et al., 2001; Kim et al., 2001; Kwak et al., 2002). The details of the upstream signaling mechanism responsible for regulating oxidative stress remain to be defined. Most studies have suggested that oxidative stress may evoke the induction of Nrf-2 or NF-κB *via* basal signal transduction systems, such as the mitogen-activated protein (MAP) kinase cascade (Kyriakis and Avruch, 2001; Takeda et al., 2003). Therefore, the upstream signaling mechanism responsible for regulating oxidative stress was studied by focusing on the MAP kinase cascades, such as extracellular signal-regulating kinase (ERK), p38 and c-Jun N-terminal kinase (JNK). The MAP kinase cascades are multi-functional signaling pathways, which are evolutionally well conserved in all eukaryotic cells. Three MAP kinase cascades that converge on ERKs, JNKs and p38 MAP kinases have already been characterized (Kyriakis and Avruch, 2001; Takeda et al., 2003). Two of these MAP kinase cascades converge on JNKs and p38 MAP kinases, and are preferentially activated by cytotoxic stresses, such as X-ray/UV irradiation, heat/osmotic shock and oxidative/nitrosative stress (Hagemann and Blank, 2001; Qadri et al., 2004; Camacho-Barquero et al., 2007).

To investigate the relationship between the physico-chemical properties and toxicities, characterization of the silica nanoparticles was performed using Branauer, Emmett and Teller (BET), transmission electron microscopy (TEM) and dynamic light scattering (DLS) methods, which provided information on the nanoparticles surface area, morphological shape and size distribution, respectively.

2. Materials and methods

2.1. Cell culture and silica nanoparticles

Human bronchial epithelial cells, Beas-2B, were purchased from the American type culture collection (ATCC, Manassas, VA, USA) and maintained in DMEM/F12 (GIBCO BRL Life Technologies, Rockville, MD, USA), supplemented with 10% (v/v) fetal bovine serum and 1% antibiotics, at 37 °C in a humidified atmosphere of air and 5% CO_2. Fumed silica (7 nm) and porous silica (5–15 nm), from Sigma (St. Louis, MO, USA), were used for the experiment. Test solutions of silica nanoparticles were prepared in the culture medium and dispersed for 20 min using a sonicator (Branson Inc., Danbury, CT, USA) to prevent aggregation. During the testing periods, the nanoparticles suspension was stable and uniform in the culture medium. The nanoparticle concentration used in this study was 1 mg/L, which prevented aggregation and/or precipitation of the particles. At this concentration, no precipitation of silica nanoparticles in the test medium occurred during the exposure period, but did at higher concentrations (data not shown). Prior to the toxicological analysis, a confocal laser scanning microscope (LSM-510, Carl Zeiss, Baden-Württemberg, Germany) was used to verify the uptake of nanoparticles by the cells, where the cells were exposed to 40 mg/L of silica nanoparticles. The cells were treated with both fumed and porous silica for 24 h for the toxicological studies.

2.2. ROS measurement

To detect the generation of ROS in nanoparticles-treated cells, a fluorometric assay, using intracellular oxidation of 2,7-dichlorofluoroscein diacetate (DCFH-DA, Sigma, St. Louis, MO, USA), was performed (Elbekai and El-Kadi, 2005; Fotakis et al., 2005) with the aid of a fluorescent microscope (Nikon, Tokyo, Japan) at excitation and emission wavelengths of 485 and 530 nm, respectively.

2.3. Western blotting

Western blotting analysis was performed, as described previously (Park et al., 2006), using an enhanced chemiluminescence western blotting detection kit (Amersham, Little Chalfont, Buckinghamshire, UK). Anti-p38 monoclonal-, anti-phospho-p38 monoclonal-, anti-ERK-2 polyclonal-, anti-phospho-ERK monoclonal- and anti-Nrf-2 polyclonal antibodies were purchased from Santa Cruz biotechnology (Santa Cruz, CA, USA). Anti-JNK polyclonal-, anti-phospho-JNK monoclonal-, anti-NF-κB monoclonal- and anti-I-κB monoclonal antibodies were from Cell Signaling (Beverly, MA, USA). Anti-HO-1 monoclonal antibody was from Stressgen (Victoria, BC, Canada) and anti-Cu/Zn SOD polyclonal antibody from Biodesign (Saco, ME, USA). Anti-Rabbit, anti-mouse and anti-sheep secondary antibodies were purchased from Santa Cruz biotechnology. Three replicates for each treatment and a control were conducted for the western blot analysis. Following the Western blotting, the relative densities of the protein bands were determined using an image analyzer, the Gel Documentation system (Vilber Lourmat TFX-20.M, Marne la Vallee, France), coupled to a Kodak 1D 3.6 camera (Kodak EDAS 290, Rochester, NY, USA).

2.4. Cell viability

The cell viability was measured using 3-[4,5-dimethylthiazol-2-yl]-2,5-di phenyltera zolium bromide (MTT) reagent (Mosmann, 1983) with a 96-well plate reader (TECAN, Hombrechtikon, Switzerland). Propidium iodide (PI) stained cells were analyzed using a flow cytometer (BD Science, San Jose, CA, USA) (Nicoletti et al., 1991). The effect on apoptosis was determined by the increase in the proportion of subG1 hypo-diploid cells.

2.5. Characterization of silica nanoparticles

To measure the surface area, the BET method was used employing a BELSORP-mini II, a volumetric adsorption apparatus (BEL Japan Inc., Osaka, Japan). To investigate the size and shape of the silica nanoparticles, 20 μl of the particle suspension in the test medium was dried on a 400 mesh carbon-coated copper grid and imaged with a JEM 1010 TEM (JEOL, Tokyo, Japan) at 40–100 kV. The size distribution of the nanoparticles was evaluated using a photal DLS spectrometer, DLS-7000 (Otsuka Electronics Co., Inc., Osaka, Japan).

2.6. Data analysis

Statistical differences between the control and treated cells were examined with the aid of an ANOVA analysis, using SPSS

12.0KO (SPSS Inc., Chicago, Il, USA). An alpha level of 0.05 was used to determine significance in all statistical analyses.

3. Results

Prior to the study on oxidative stress, the incorporation of silica nanoparticles into the cells was examined using confocal LSM (Fig. 1). The confocal LSM images showed that the silica nanoparticles were incorporated into the cells and distributed around the nucleus area, which was more obvious with porous silica than with fumed silica. The temporal formation of ROS was visualized in Beas-2B cells exposed to silica nanoparticles by inspection under fluorescent microscope (Fig. 2). DCFH-DA staining revealed an increased ROS concentration in the silica treated cells; however, a quantification analysis did not indicate any difference between the two types of nanoparticle. The formation of ROS continued to increase up to 24 h in both types of silica. With the observed increase in the formation of ROS, markers for cellular defense mechanism against oxidative stress (i.e. induction of antioxidant enzymes) were investigated in Beas-2B cells exposed to silica nanoparticles (Fig. 3). The expression of SOD protein was unchanged, whereas that of HO-1 was increased by both fumed and porous silica nanoparticles.

With the increased formation of ROS and the induction of antioxidant enzyme, HO-1, were observed on exposure to silica nanoparticles, and redox-sensitive transcription factors, NF-κB and Nrf-2 were examined in the cytosolic and nuclear fraction of cells treated with silica nanoparticles. Neither nuclear localization of NF-κB nor the degradation of cytosolic I-κB was observed, whereas expression of Nrf-2 in the nuclear fraction increased in cells treated with silica nanoparticles (Fig. 4). Nuclear localization of Nrf-2 was greater in the cells exposed to porous silica than in those to fumed silica.

To further clarify the possible upstream oxidative signaling pathway involved in Nrf-2 activation, leading to HO-1 induction, the activation of MAP kinases was examined, known as major signaling kinases involved in cell survival against oxidative stress through the Nrf-2 signaling pathway (Fig. 5). The expressions of the unphosphorlyated forms of MAP kinases were constant, regardless of exposure of silica nanoparticles; whereas, the expression of the phosphorylated form of ERK was strongly induced by silica nanoparticles. There was significant phosphorylation of ERK by exposure to both porous and fumed silica (about 5 to 8-fold compared with that of the control). The expression level of phosphorylated p38 or JNK was unchanged by exposure to silica nanoparticles.

To investigate silica nanoparticles-induced oxidative stress (ROS formation and induction of antioxidant enzymes) lead cellular consequences, cell viability and apoptosis were examined (Table 1). About 80% of cell viability was observed in silica exposed cells compared to that in the control. Flow cytometry analysis was conducted using PI staining to quantify the number of cells with a subdiploid DNA content. In the cells exposed to porous silica nanoparticles, the numbers of cells with a subdiploid DNA content increased about 3-fold compared to that in the control.

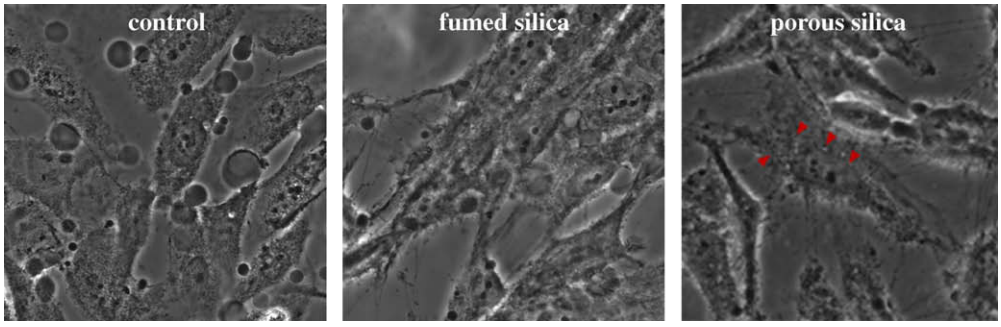

Fig. 1. Confocal phase contrast image observed in Beas-2B cells exposed to fumed silica and porous silica nanoparticles for 24 h. Aggregates of silica nanoparticles in the cells were visualized using confocal LSM.

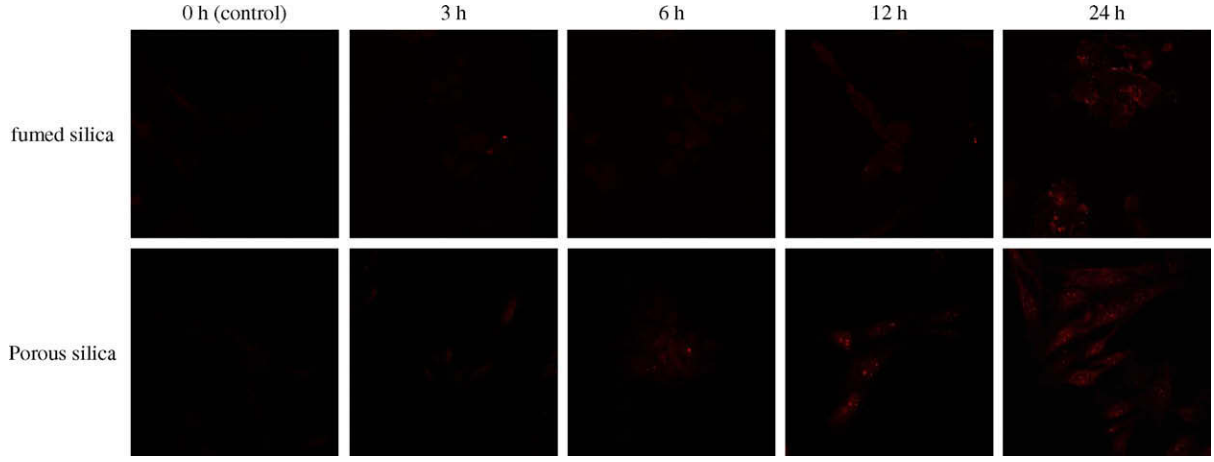

Fig. 2. ROS induced by fumed silica and porous silica nanoparticles in Beas-2B cells. The cells exposed to nanoparticles for 0, 3, 6, 12 and 24 h were incubated with 40 μM DCFH-DA at 37 °C for 30 min and were observed under fluorescence microscope.

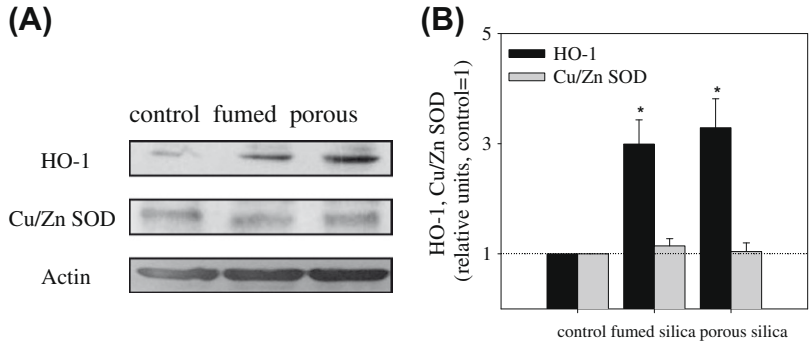

Fig. 3. Expression of HO-1 and Cu/Zn SOD in Beas-2B cells exposed to fumed silica and porous silica nanoparticles for 24 h (A). Densitometric values of expression of HO-1 and Cu/Zn SOD were normalized using that of Actin and were presented as relative units compared to control. Data represent the mean ± standard error of the mean of three individual experiments. $^{*}p < 0.05$ compared to control group (B).

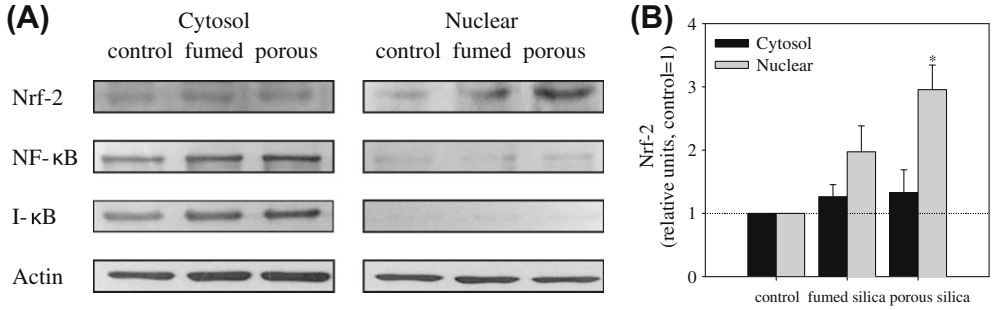

Fig. 4. Expression of NF-κB, I-κB and Nrf-2 in cytosolic and nuclear fraction of Beas-2B cells exposed to fumed silica and porous silica nanoparticles for 24 h (A). Densitometric values of expression of Nrf-2 were normalized using that of Actin and were presented as relative units compared to control. Data represent the mean ± standard error of the mean of three individual experiments. $^{*}p < 0.05$ compared to control group (B).

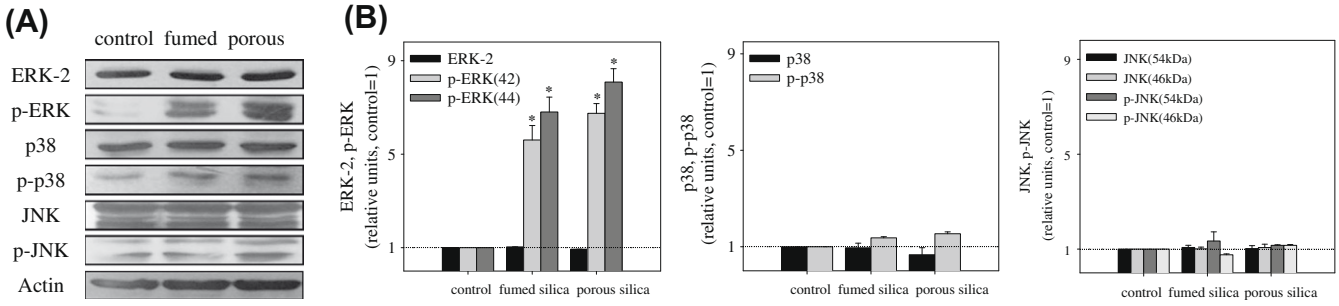

Fig. 5. Expression of intact and phosphorylated ERK, p38 and JNK in Beas-2B cells exposed to fumed silica and porous silica nanoparticles for 24 h (A). Densitometric values of expression of ERK, p38 and JNK were normalized using that of Actin and were presented as relative units compared to control. Data represent the mean ± standard error of the mean of three individual experiments. $^{*}p < 0.05$ compared to control group (B).

The results of the overall oxidative study showed that the expressions of HO-1, p-ERK and nuclear Nrf-2, as well as the numbers of cells with a subdiploid DNA content, increased more significantly with exposure to porous than fumed silica. To understand this different sensitivity between the two types of silica nanoparticle, the physico-chemical properties of silica nanoparticles were characterized using BET, TEM and DLS methods (Fig. 6). The BET surface areas of fumed- and porous silica were 349.71 and 644.44 m^3/g, respectively. The TEM images of the silica nanoparticles in the test medium showed different morphologies of the nanoparticles. The size distribution in the test medium was investigated using a DLS method, which showed that the nanoparticles exposed to the cells did not exist as single particles, but tended to aggregate in the test medium, as the size of the nanoparticles distributed in the test medium were about 400 and 20 nm, for fumed- and porous silica nanoparticles, respectively.

4. Discussions

Numerous studies on nanoparticle toxicity have dealt with oxidative stress (Shvedova et al., 2003; Xia et al., 2004; Green and Howman, 2005; Hussain et al., 2005; Sayes et al., 2005; Foster et al., 2006; Lin et al., 2006; Limbach et al., 2007; Monteiller et al., 2007). However, the mechanism by which oxidative stress is involved in nanotoxicity has been poorly addressed. In this study, cells were treated with a constant concentration of different

Table 1
Cell viability and the apoptosis investigated in the cells exposed to fumed silica and porous silica nanoparticles (mean ± standard error of the mean; number = 3, $^{*}p < 0.05$).

	Control	Fumed silica	Porous silica
Cell viability	1.000 ± 0.019	0.839 ± 0.009	0.799 ± 0.014*
SubG1 (%)	3.30 ± 1.07	6.45 ± 0.64	12.41 ± 0.58*
G1 (%)	43.53 ± 0.83	45.85 ± 0.94	46.81 ± 2.79
S (%)	33.71 ± 0.65	34.15 ± 1.37	34.76 ± 1.25
G2 (%)	22.76 ± 1.48	20.00 ± 0.43	18.43 ± 1.54

The cell viability was measured using MTT assay (control = 1). The apoptosis was investigated by quantifying the number of cells with a subdiploid DNA contents (subG1) using flow cytometry.

types of silica nanoparticle. Direct measurement of the ROS, as well as the induction of antioxidant enzyme (Figs. 2 and 3), provided strong evidence for the involvement of oxidative stress in silica nanoparticles-induced toxicity. To understand the mechanism of the observed silica nanoparticles-induced oxidative stress, the activation of transcription factors (i.e. NF-κB, Nrf-2) and the signal transduction pathway responding to oxidative stress (i.e. MAP kinase pathway) were investigated.

In our study, silica nanoparticles induced the translocation of Nrf-2 into the nucleus, as evidenced by the results of the western blot analysis (Fig. 4). The translocation of Nrf-2 into the nucleus following nanoparticle treatments was associated with an increase in HO-1 protein, which suggests that porous nanoparticles activate Nrf-2 in association with the upregulation of HO-1 in Beas-2B cells. However, in this study, no NF-κB activation on exposure to silica nanoparticles occurred, which was also observed in our previous study with synthesized ceria nanoparticles (Eom and Choi, 2009). However, to confirm silica nanoparticles-induced activation of transcription factor, more direct evidence, such as data from an electrophoretic mobility shift assay may be needed.

The activation of the ERK MAP kinase pathway by silica nanoparticles suggests that the induction of HO-1 may be mediated through the Nrf-2–ERK MAP kinase signaling pathway. ERK has been known to respond to internal stimuli, such as growth factors, however, our study revealed that silica nanoparticles strongly induce the phosphorylation of ERK (Fig. 5). The activation of the ERK signaling pathway by environmental stimuli, such as cadmium, oil fly ash, phorbol myristate acetate and UVA, has already been reported, which suggest that the ERK signaling pathway also responds to environmental stressors (Roberts et al., 2003; Liu et al., 2004; Whitehurst et al., 2004; Kim and Sharma, 2006). The present study using silica nanoparticles provides more evidence that the ERK pathway might respond to environmental stimuli; however, the mechanism by which this response occurred merits further investigation. Especially, how MAP kinase signaling pathways are involved in cellular defense mechanisms toward exposure to different types of nanoparticle would be an interesting research topic in the emerging field of nanotoxicity. Indeed, our previous study with a similar experimental scheme, but different nanoparticles, ceria, showed activation of p38 kinase, but not ERK. The overall results on ceria nanoparticles suggest that ceria may exert their toxicity through oxidative stress, as they cause significant increases in the cellular ROS concentrations, subsequently leading to the strong induction of HO-1 *via* the p38-Nrf-2 signaling pathway (Eom and Choi, 2009).

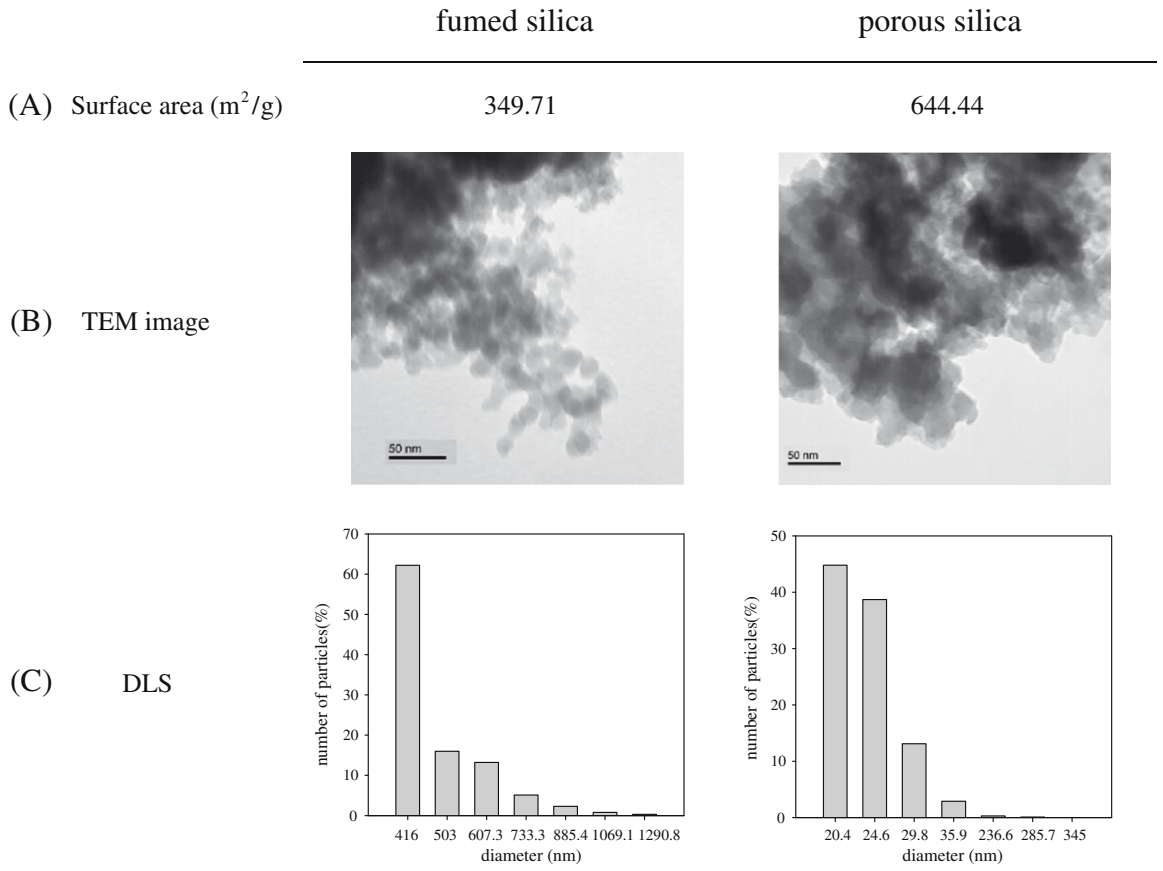

Fig. 6. Characterization of fumed silica and porous silica nanoparticles using BET, TEM and DLS methods. Surface areas of nanoparticles were measured using BET method (A), particles shape were analysed by TEM (B) and the size distribution in the test media were evaluated by DLS (C).

Oxidative stress biomarkers, such as, DNA damage, lipid peroxidation, antioxidant enzyme activities, can be used to assess changes at cellular levels; therefore, in this study, to provide insights into the relative sensitivity and cellular consequences of the oxidative stress response observed in Figs. 2–5, cytotoxicity tests were conducted (Table 1). Exposure to silica nanoparticles seemed to slightly affect the cell viability. The relationships between oxidative stress responses and cellular consequences are complicated due to the compensatory mechanisms regulating cellular fitness. As oxidative stress is potentially implicated in many human diseases, a sensitive and rapid method for the detection of a property of oxidative stress due to exposure to nanoparticles is considered important, although it does not necessarily include severe cellular level alteration. Nevertheless, the oxidative stress parameters tested in this study were rather limited in terms of allowing a full understanding of oxidative stress and the cellular response due to exposure to silica nanoparticles. If further cellular parameters in the involvement of the observed oxidative stress response, such as DNA fragmentation, chromosome condensation and caspase activity, with various exposure periods, had been tested, the physiological pathway could probably have been more clearly evaluated and explained. Further studies on the mechanism by which silica nanoparticles induce the Nrf-2–ERK MAP kinase pathway, to gain a better understand nanoparticles-induced oxidative stress, as well as studies on the relationship between physico-chemical properties of nanoparticles and cytotoxicity, are warranted.

The overall results showed that the expressions of ERK and nuclear Nrf-2, and the numbers of cells with DNA contents in subG1 phase, increased more significantly with porous than fumed silica, which suggests porous silica might have greater toxicity potential than fumed silica. With nanoparticle toxicity, it is often expected that the smaller the size, the stronger the exerted toxicity (Oberdörster et al., 2005); however, the relationship between the physico-chemical properties of nanoparticles and their toxicities seems to be much more complicated than just a matter of their size and surface area (i.e. shape, charge, concentration, etc.), but the debate is still on going (Hussain et al., 2005; Sayes et al., 2006; Fujiwara et al., 2008). Indeed, many studies have failed to show any clear relationship between cytotoxicity and nanoparticle size (Hussain et al., 2005; Yin et al., 2005). Preparation, dosing and maintenance of nanoparticles within the test medium are important factors when investigating the potential harmful effect of nanoparticles exposure and, among the various physico-chemical properties of nanoparticles, the aggregation process is an important factor influencing toxicity. In this study, the characterizations of silica nanoparticles in test medium as well as their influence on cytotoxicity were investigated (Fig. 6). As silica nanoparticles exist both individually and in aggregates, their states in the test media were characterized by TEM, to determine the size and the state of the silica nanoparticles. The TEM provided information on the size and shape of nanoparticles; however, it could not provide information on whether the nanoparticles existed in single or aggregated forms in the test medium, as the nanoparticles form aggregates when dried on the microscopic observation slide. The DLS and BET result revealed that the fumed silica nanoparticles did not exist as single particles, but tended to aggregate in the test medium, whereas, porous silica nanoparticles exist as single particles, which suggest that the toxicity of nanoparticles may be related with the surface area, as there was a significant difference in the surface areas (349.71 and 644.44 m^3/g) between fumed- and porous silica nanoparticles. However, the lines of evidence provided from the present study are rather limited; therefore, to identify key properties of nanoparticles causing toxicity, the toxic responses to a broad range of physico-chemical properties to various classes of nanoparticles may be investigated in various cell types.

Conflict of interest statement

The authors declare that there are no conflicts of interest.

Acknowledgment

This subject is supported by Korea Ministry of Environment as "The Eco-technopia 21 project".

References

Bharali, D.J., Klejbor, I., Stachowiak, E.K., Dutta, P., Roy, I., Kaur, N., Bergey, E.J., Prasad, P.N., Stachowiak, MK., 2005. Organically modified silica nanoparticles: a nonviral vector for in vivo gene delivery and expression in the brain. Proc. Natl. Acad. Sci. USA 102, 11539–11544.

Camacho-Barquero, L., Villegas, I., Sánchez-Calvo, J.M., Talero, E., Sánchez-Fidalgo, S., Motilva, V., Alarcón de la Lastra, C., 2007. Curcumin, a Curcuma longa constituent, acts on MAPK p38 pathway modulating COX-2 and iNOS expression in chronic experimental colitis. Int. Immunopharmacol. 7, 333–342.

Chan, K., Han, X.D., Kan, Y.W., 2001. An important function of Nrf2 in combating oxidative stress: detoxification of acetaminophen. Proc. Natl. Acad. Sci. USA 98, 4611–4616.

Chan, K., Kan, Y.W., 1999. Nrf2 is essential for protection against acute pulmonary injury in mice. Proc. Natl. Acad. Sci. USA 96, 12731–12736.

Eom, H.J., Choi, J., 2009. Oxidative stress of CeO_2 nanoparticles via p38-Nrf-2 signaling pathway in human bronchial epithelial cell, Beas-2B. Toxicol. Lett., doi:10.1016/j.toxlet.2009.01.028.

Elbekai, R.H., El-Kadi, A.O., 2005. The role of oxidative stress in the modulation of aryl hydrocarbon receptor-regulated genes by As^{3+}, Cd^{2+}, and Cr^{6+}. Free Radic. Biol. Med. 39, 1499–1511.

Foster, K.A., Galeffi, F., Gerich, F.J., Turner, D.A., Muller, M., 2006. Optical and pharmacological tools to investigate the role of mitochondria during oxidative stress and neurodegeneratation. Prog. Neurobiol. 79, 136–171.

Fotakis, G., Cemeli, E., Anderson, D., Timbrell, J.A., 2005. Cadmium chloride-induced DNA and lysosomal damage in a hepatoma cell line. Toxicol. in Vitro 19, 481–489.

Fujiwara, K., Suematsu, H., Kiyomiya, E., Aoki, M., Sato, M., Moritoki, N., 2008. Size-dependent toxicity of silica nano-particles to Chlorella kessleri. J. Environ. Sci. Health A Tox. Hazard Subst. Environ. Eng. 43, 1167–1173.

Gemeinhart, R.A., Luo, D., Saltzman, W.M., 2005. Cellular fate of a modular DNA delivery system mediated by silica nanoparticles. Biotechnol. Prog. 21, 532–537.

Green, M., Howman, E., 2005. Semiconductor quantum dots and free radical induced DNA nicking. Chem. Commun. 121, 121–123.

Hagemann, C., Blank, J.L., 2001. The ups and downs of MEK kinase interactions. Cell Signal. 13, 863–875.

Handy, R.D., Owen, R., Valsami-Jones, E., 2008. The ecotoxicology of nanoparticles and nanomaterials: current status, knowledge gaps, challenges, and future needs. Ecotoxicology 17, 315–325.

Hayes, J.D., Chanas, S.A., Henderson, C.J., McMahon, M., Sun, C., Moffat, G.J., Wolf, C.R., Yamamoto, M., 2000. The Nrf2 transcription factor contributes both to the basal expression of glutathione S-transferases in mouse liver and to their induction by the chemopreventive synthetic antioxidants, butylated hydroxyanisole and ethoxyquin. Biochem. Soc. Trans. 28, 33–41.

Hirsch, L.R., Stafford, R.J., Bankson, J.A., Sershen, S.R., Rivera, B., Price, R.E., Hazle, J.D., Halas, N.J., West, J.L., 2003. Nanoshell-mediated near-infrared thermal therapy of tumors under magnetic resonance guidance. Proc. Natl. Acad. Sci. USA 100, 13549–13554.

Hoet, P.H.M., Brüske-Hohlfeld, I., Salata, O.V., 2004. Nanoparticles–known and unknown health risks. J. Nanobiotechnol. 2, 12.

Hussain, S.M., Hess, K.L., Gearhart, J.M., Geiss, K.T., Schlager, J.J., 2005. In vitro toxicity of nanoparticles in BRL 3A rat liver cells. Toxicol. in Vitro 19, 975–983.

Itoh, K., Chiba, T., Takahashi, S., Ishii, T., Igarashi, K., Katoh, Y., Oyake, T., Hayashi, N., Satoh, K., Hatayama, I., Yamamoto, M., Nabeshima, Y., 1997. An Nrf2/small Maf heterodimer mediates the induction of phase II detoxifying enzyme genes through antioxidant response elements. Biochem. Biophys. Res. Commun. 236, 313–322.

Janssen, Y.M., Barchowsky, A., Treadwell, M., Driscoll, K.E., Mossman, B.T., 1995. Asbestos induces nuclear factor kappa B (NF-kappa B) DNA-binding activity and NF-kappa B-dependent gene expression in tracheal epithelial cells. Proc. Natl. Acad. Sci. USA 92, 8458–8462.

Kaewamatawong, T., Shimada, A., Okajima, M., Inoue, H., Morita, T., Inoue, K., Takano, H., 2006. Acute and subacute pulmonary toxicity of low dose of ultrafine colloidal silica particles in mice after intratracheal instillation. Toxicol. Pathol. 34, 958–965.

Kim, J., Sharma, R.P., 2006. Cadmium-induced apoptosis in murine macrophages is antagonized by antioxidants and caspase inhibitors. J. Toxicol. Environ. Health A 69, 1181–1201.

Kim, Y.C., Masutani, H., Yamaguchi, Y., Itoh, K., Yamamoto, M., Yodoi, J., 2001. Hemin-induced activation of the thioredoxin gene by Nrf2. A differential regulation of the antioxidant responsive element by a switch of its binding factors. J. Biol. Chem. 276, 18399–18406.

Kwak, M.K., Itoh, K., Yamamoto, M., Kensler, T.W., 2002. Enhanced expression of the transcription factor Nrf2 by cancer chemopreventive agents: role of antioxidant response element-like sequences in the nrf2 promoter. Mol. Cell Biol. 22, 2883–2892.

Kyriakis, J.M., Avruch, J., 2001. Mammalian mitogen-activated protein kinase signal transduction pathways activated by stress and inflammation. Physiol. Rev. 81, 807–869.

Limbach, L.K., Wick, P., Manser, P., Grass, R.N., Bruinink, A., Stark, W.J., 2007. Exposure of engineered nanoparticles to human lung epithelial cells: influence of chemical composition and catalytic activity on oxidative stress. Environ. Sci. Technol. 41, 4158–4163.

Lin, W., Huang, Y.W., Zhou, X.D., Ma, Y., 2006. In vitro toxicity of silica nanoparticles in human lung cancer cells. Toxicol. Appl. Pharmacol. 217, 252–259.

Liu, J.P., Schlosser, R., Ma, W.Y., Dong, Z., Feng, H., Liu, L., Huang, X.Q., Liu, Y., Li, D.W., 2004. Human alphaA- and alphaB-crystallins prevent UVA-induced apoptosis through regulation of PKCalpha, RAF/MEK/ERK and AKT signaling pathways. Exp. Eye Res. 79, 393–403.

Lu, J., Liong, M., Zink, J.I., Tamanoi, F., 2007. Mesoporous silica nanoparticles as a delivery system for hydrophobic anticancer drugs. Small 3, 1341–1346.

Monteiller, C., Tran, L., MacNee, W., Faux, S., Jones, A., Miller, B., Donaldson, K., 2007. The pro-inflammatory effects of low-toxicity low-solubility particles, nanoparticles and fine particles, on epithelial cells in vitro: the role of surface area. Occup. Environ. Med. 64, 609–615.

Mosmann, T., 1983. Rapid colorimetric assay for cellular growth and survival: application to proliferation and cytotoxicity assays. J. Immunol. Meth. 16, 55–63.

Nel, A., Xia, T., Mädler, L., Li, N., 2006. Toxic potential of materials at the nanolevel. Science 311, 622–627.

Nicoletti, I., Migliorati, G., Pagliacci, M.C., Grignani, F., Riccardi, C., 1991. A rapid and simple method for measuring thymocyte apoptosis by propidium iodide staining and flow cytometry. J. Immunol. Meth. 139, 271–279.

Nohynek, G.J., Lademann, J., Ribaud, C., Roberts, M.S., 2007. Grey goo on the skin? Nanotechnology, cosmetic and sunscreen safety. Crit. Rev. Toxicol. 37, 251–277.

Oberdörster, G., Oberdörster, E., Oberdörster, J., 2005. Nanotoxicology: an emerging discipline evolving from studies of ultrafine particles. Environ. Health Perspect. 113, 823–839.

Pinkus, R., Weiner, L.M., Daniel, V., 1996. Role of oxidants and antioxidants in the induction of AP-1, NF-kappaB, and glutathione S-transferase gene expression. J. Biol. Chem. 271, 13422–13429.

Qadri, I., Iwahashi, M., Capasso, J.M., Hopken, M.W., Flores, S., Schaack, J., Simon, F.R., 2004. Induced oxidative stress and activated expression of manganese superoxide dismutase during hepatitis C virus replication: role of JNK, p38 MAPK and AP-1. Biochem. J. 378, 919–928.

Qhobosheane, M., Santra, S., Zhang, P., Tan, W., 2001. Biochemically functionalized silica nanoparticles. Analyst 126, 1274–1278.

Roberts, E.S., Richards, J.H., Jaskot, R., Dreher, K.L., 2003. Oxidative stress mediates air pollution particle-induced acute lung injury and molecular pathology. Inhal. Toxicol. 15, 1327–1346.

Rogueda, P.G., Traini, D., 2007. The nanoscale in pulmonary delivery. Part 1: deposition, fate, toxicology and effects. Expert Opin. Drug Deliv. 4, 595–606.

Santra, S., Zhang, P., Wang, K., Tapec, R., Tan, W., 2001. Conjugation of biomolecules with luminophore-doped silica nanoparticles for photostable biomarkers. Anal. Chem. 73, 4988–4993.

Sayes, C.M., Gobin, A.M., Ausman, K.D., Mendez, J., West, J.L., Colvin, V.L., 2005. Nano-C_{60} cytotoxicity is due to lipid peroxidation. Biomaterials 26, 7587–7595.

Sayes, C.M., Wahi, R., Kurian, P.A., Liu, Y., West, J.L., Ausman, K.D., Warheit, D.B., Colvin, V.L., 2006. Correlating nanoscale titania structure with toxicity: a cytotoxicity and inflammatory response study with human dermal fibroblasts and human lung epithelial cells. Toxicol. Sci. 92, 174–185.

Sen, C.K., Packer, L., 1996. Antioxidant and redox regulation of gene transcription. FASEB J. 10, 709–720.

Shvedova, A.A., Castranova, V., Kisin, E.R., Schwegler-Berry, D., Murray, A.R., Gandelsman, V.Z., Maynard, A., Baron, P.J., 2003. Exposure to carbon nanotube material: assessment of nanotube cytotoxicity using human keratinocyte cells. Toxicol. Environ. Health 66, 1909–1926.

Takeda, K., Matsuzawa, A., Nishitoh, H., Ichijo, H., 2003. Roles of MAPKKK ASK1 in stress-induced cell death. Cell Struct. Funct. 28, 23–29.

Venkatesan, N., Yoshimitsu, J., Ito, Y., Shibata, N., Takada, K., 2005. Liquid filled nanoparticles as a drug delivery tool for protein therapeutics. Biomaterials 26, 7154–7163.

Warheit, D.B., Hoke, R.A., Finlay, C., Donner, E.M., Reed, K.L., Sayes, C.M., 2007. Development of a base set of toxicity tests using ultrafine TiO_2 particles as a component of nanoparticle risk management. Toxicol. Lett. 171, 99–110.

Whitehurst, A., Cobb, M.H., White, M.A., 2004. Stimulus-coupled spatial restriction of extracellular signal-regulated kinase 1/2 activity contributes to the specificity of signal-response pathways. Mol. Cell Biol. 24, 10145–10150.

Xia, T., Korge, P., Weiss, J.N., Li, N., Venkatesen, M.I., Sioutas, C., Nel, A., 2004. Quinones and aromatic chemicals compounds inparticulate matter induce mitochondrial dysfunction: implications for ultrafine particle toxicity. Environ Health Perspect. 112, 1347–1358.

Yin, H., Too, H.P., Chow, G.M., 2005. The effects of particle size and surface coating on the cytotoxicity of nickel ferrite. Biomaterials 26, 5818–5826.

Zhang, F.F., Wan, Q., Li, C.X., Wang, X.L., Zhu, Z.Q., Xian, Y.Z., Jin, L.T., Yamamoto, K., 2004. Simultaneous assay of glucose, lactate, L-glutamate and hypoxanthine levels in a rat striatum using enzyme electrodes based on neutral red-doped silica nanoparticles. Anal. Bioanal. Chem. 380, 637–642.

Zhao, J., Wu, P., Brancewicz, C., Li, Y., 2007. A liposome-containing slurry for tungsten chemical mechanical polishing. J. Electrochem. Soc. 154, 225–230.